Journal of Hazardous Materials 170 (2009) 954–961

Contents lists available at ScienceDirect

Journal of Hazardous Materials

journal homepage: www.elsevier.com/locate/jhazmat

Minimization of organic content in simulated industrial wastewater by Fenton type processes: A case study

Ivana Grčić[a], Dinko Vujević[a], Josip Šepčić[b], Natalija Koprivanac[a,*]

[a] Department of Polymer Engineering and Organic Chemical Technology, Faculty of Chemical Engineering and Technology, University of Zagreb, Marulićev trg 19, HR-10000 Zagreb, Croatia
[b] DINA Petrokemija Inc., Bjanižov 1, HR-51513 Omišalj, Croatia

ARTICLE INFO

Article history:
Received 6 April 2009
Received in revised form 13 May 2009
Accepted 14 May 2009
Available online 21 May 2009

Keywords:
Industrial wastewater treatment
Advanced oxidation processes (AOPs)
Fenton type processes
Box–Behnken design (BBD)
Desirability function approach (DFA)

ABSTRACT

Pre-treatment of simulated industrial wastewaters (SIM1, SIM2 and SIM3) containing organic and inorganic compounds (1,2-dichloroethane, sodium formate, sodium hydrogen carbonate, sodium carbonate and sodium chloride) by oxidative degradation using homogeneous Fenton type processes (Fe^{2+}/H_2O_2 and Fe^{3+}/H_2O_2) has been evaluated. The effects of initial Fe^{2+} and Fe^{3+} concentrations, [$Fe^{2+/3+}$], type of iron salt (ferrous sulfate vs. ferric chloride), initial hydrogen peroxide concentration, [H_2O_2], on mineralization extent, i.e., total organic content (TOC) removal, were studied. Response surface methodology (RSM), particularly Box–Behnken design (BBD) was used as modelling tool, and obtained predictive function was used to optimize the overall process by the means of desirability function approach (DFA). Up to 94% of initial TOC was removed after 120 min. Ferrous sulfate was found to be the most appropriate reagent, and the optimal doses of Fe^{2+} and H_2O_2 for reducing the pollutant content, in terms of final TOC and sludge production were assessed.

1. Introduction

The increasing growth of world's population and rapid industrial development cause the formation of the huge amount of wastewater loaded with the numerous organic compounds unacceptable for the environment and human health as well. In order to preserve the environment, following the principles of cleaner production and sustainable development, removal of toxic and hazardous compounds from industrial wastewater presents a great issue. New directives and regulations demand the necessity for finding the optimal solution of the treatment of such wastewater, in order to decrease concentration of hazardous compounds bellow the maximal concentration prescribed by the regulation. The purification of wastewater has been conducted in order to protect natural resources and enable the possibility of reuse of this water, saving the fresh and natural water in the same time, as the priority of sustainable development and environmental protection. In general, methods for the industrial wastewater treatment can be grouped as biological, physical and chemical methods [1]. Biological methods have the widespread use for the treatment of municipal and industrial wastewater. Despite of the lot of advantages, some pollutants, including the most toxic organic compounds cannot be destroyed by biological degradation processes because of their low biodegradability. Physical methods of wastewater treatment generally present transfer of pollution from one phase to the other, often expensive and not eco-efficient. Also, a secondary waste disposal and adsorbent regeneration additionally decrease the economical efficiency of wastewater treatment by physical methods. An alternative to the conventional wastewater treatment processes presents advanced oxidation processes (AOPs) that can be applied individually or as a part of integral treatment process. The advantage of these processes in comparison with conventional wastewater treatment methods is the possibility of the complete degradation of organic load towards water and carbon dioxide. AOPs include the formation of highly reactive species (radicals) under the chemical, electrical or radioactive energy and they can react non-selectively with persistent organic compounds transferring them into by-products which can be degraded much more easily [2]. These intermediates have high oxidation potential and one of the most important is hydroxyl radical (2.8 eV). It can attack and destruct organic compounds towards water and carbon dioxide, i.e., mineralization [3–5].

In order to obtain the balance between economical growth and development, legislative and healthy environment and driven by the desire for preserving of the beautiful local environment and ecosystem, an application of new technologies need to be studied for possible implementation in industrial wastewater treatment. Among all kind of industrial wastewaters, those ones originating from petrochemical industries are considered as very complex and hard to treat. The constituents of the petrochemical wastewaters are

* Corresponding author. Tel.: +385 1 4597 123; fax: +385 1 4597 143.
E-mail address: nkopri@fkit.hr (N. Koprivanac).

0304-3894/$ – see front matter © 2009 Elsevier B.V. All rights reserved.
doi:10.1016/j.jhazmat.2009.05.060

highly specific. Therefore, each wastewater has to be characterized extensively and viable processing technologies have to be evaluated for the treatment.

Oxidative degradation by using Fenton process appeared to be efficient for the treatment of wastewaters even at higher initial organic content [6,7]. Fenton process is based on the oxidation with Fenton reagent which presents an oxidative mixture of hydrogen peroxide and ferrous ions (Fe^{2+}) as catalyst. In general, the efficiency of Fenton process depends on: concentration of ferrous (Fe^{2+}) and hydrogen peroxide Eq. (1), their molar ratio, pH of the system and temperature [8,9].

$$Fe^{2+} + H_2O_2 \rightarrow Fe^{3+} + HO^- + HO^\bullet \quad (1)$$

Decomposition of hydrogen peroxide can be also catalyzed by ferric ions, Fe^{3+}, Eqs. (2) and (3).

$$Fe^{3+} + H_2O_2 \rightarrow Fe^{2+} + HO_2^\bullet \quad (2)$$

$$Fe^{3+} + HO_2^\bullet \rightarrow Fe^{2+} + H^+ + O_2 \quad (3)$$

Previous Fenton studies have shown that acidic pH levels near 3 are usually optimum for Fenton oxidations. The ferrous ions generated in the above reactions react with hydroxide ions to form ferric hydroxo complexes [10].

Within pH 3 and 7, the above complexes become "larger" which accounts for the coagulation capability of Fenton's reagent and easier precipitation. It should be noted that large amounts of small flocs are consistently observed in the Fenton oxidation step [6,10].

In this particular system, the carboxyl radical, $CO_2^{\bullet-}$, is also one of the most important species because of its excellent reducing properties (−1.9 eV) [11]. This radical reacts very rapidly with many compounds [12]. It may be easily produced by the reactions of hydroxyl radical and H atom with formic acid/formate as shown below [13]:

$$HO^\bullet + HCO_2^- \rightarrow H_2O + CO_2^{\bullet-} \quad (4)$$

The $CO_2^{\bullet-}$ radical is presented in this form throughout most of the pH range and only protonated in strongly acidic solution. It is suggested [14] that an intermediate of the recombination of $CO_2^{\bullet-}$ radicals [$CO_2^{\bullet-}\cdots CO_2^{\bullet-}$] was produced. This intermediate can either lead to the formation of stable products such as oxalate and CO_2 or dissociate back to $CO_2^{\bullet-}$ radicals:

$$CO_2^{\bullet-} + CO_2^{\bullet-} \leftrightarrow [CO_2^{\bullet-}\cdots CO_2^{\bullet-}] \rightarrow \text{products} \quad (5a)$$

$$[CO_2^{\bullet-}\cdots CO_2^{\bullet-}] \rightarrow \quad (5b)$$

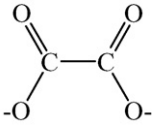

$$[CO_2^{\bullet-}\cdots CO_2^{\bullet-}] \rightarrow 2O{=}C{=}O \quad (5c)$$

The scope of this study was to investigate the efficiency of homogeneous Fenton type processes (Fe^{2+}/H_2O_2 and Fe^{3+}/H_2O_2) on simulated industrial wastewater originated from 1,2-DCA/VCM plant, and optimize the oxidation of model pollutants. An optimization strategy based on desirability function approach (DFA) together with response surface methodology (RSM) has been used. Box–Behnken experimental design was used to develop a predictive model for mineralization extent involving four independent factors. Furthermore, the single-response optimization was attempted through desirability function based on a developed predictive model. Single-response optimization means determination of the values of control factors, i.e., process parameters that gave lowest value of a particular response, final TOC content of the system, according to set criteria.

2. Materials and methods

2.1. Chemicals

All reagents used in this work were analytical or HPLC grade and used without any further purification. Ferrous sulfate ($FeSO_4{\cdot}7H_2O$), hydrogen peroxide (H_2O_2 30%), sodium hydrogen carbonate ($NaHCO_3$), sodium carbonate (Na_2CO_3), sodium chloride (NaCl), barium chloride ($BaCl_2$) and sulfuric acid (H_2SO_4) were supplied by Kemika, Zagreb, Croatia. Sodium formate (HCOONa) and ortho-phosphoric acid (H_3PO_4 85%) were obtained from Fluka. Oxalic acid ($H_2C_2O_4$) was purchased from Sigma–Aldrich, 1,2-dichlorethane (1,2-DCA) from The British Drug House Ltd., B.D.H. Laboratory Chemicals Division, Poole, United Kingdom and ferric chloride ($FeCl_3{\cdot}6H_2O$) from Riedel-de Haën AG, Seelze, Germany.

2.2. Simulated wastewater

The degradation experiments were performed with three types of simulated industrial wastewater (Table 1). Simulated wastewaters were prepared by transferring the exact amounts of HCOONa, $NaHCO_3$, NaCl and 1,2-DCA in the 1 L flask and dissolved with deionized water. The pH of the system was maintained at 10 with addition of Na_2CO_3.

2.3. Experimental procedure

All experiments were performed as jar-tests in 150 mL beakers made of borosilicate glass, with the reaction volume of 100 mL and constant magnetic stirring (600 rpm) within 120 min, at room temperature, 23 ± 2 °C. After the addition of iron catalyst, the initial pH of the studied systems was adjusted at 3.5 using of sulfuric acid (80%) [5,15,16], which was followed by the addition of hydrogen peroxide. Samples of reaction mixture after the treatment were left to sedimentation for 30 min. The volume of residual sludge (V_{30}) was measured. Where it was necessary reaction mixture was filtered using Whatman filter paper (blue stripe). The sludge was oven dried at 50 °C for 24 h, cooled off to room temperature and weighted (m_F). Solid residue, as well as each supernatant, was subjected to further analyses.

2.4. Analyses

The concentration of ferric ions in the bulk was measured by colorimetric method using the UV–vis spectrophotometer, Lambda EZ 201, Perkin Elmer, USA. Ferrous ions were identified by the reaction of Fe^{2+} with 1,10-phenantroline giving an orange–red complex (λ_{max} = 510 nm). Ferric ions were identified by the reaction of Fe^{3+} with thiocyanate forming a red-colored complex (λ_{max} = 480 nm) under acidic conditions [17]. The concentration of H_2O_2 was determined by using the procedure described in the literature [18]. The method is based on the reaction of H_2O_2 with ammonium metavanadate in acidic medium, which results in the formation of a red–orange color peroxovanadium cation, with maximum absorbance at 450 nm and its formation was also monitored by

Table 1
Characteristics of studied simulated systems.

System	SIM1	SIM2	SIM3
w(HCOONa), %	0.1	0.8	1.5
γ(1,2-DCA), mg L^{-1}	20	20	20
w($NaHCO_3$), %	7.0	7.0	7.0
w(NaCl), %	4.5	4.5	4.5
pH	10	10	10
TOC, mg L^{-1}	370	2930	5500

the same UV–vis spectrophotometer. Organic and inorganic content in the samples were measured on the basis of TOC and IC measurements performed by using a Shimadzu, Japan TOC V_{CPN} 5000 A analyzer. Concentration of formic and oxalic acid in supernatant was determined using High Performance Liquid Chromatographer HPLC, Shimadzu, with SUPELCOGEL H Carbohydrate column, length 250 mm, internal diameter 4.6 mm and UV detection at 210 nm. The mobile phase was 0.1% phosphoric acid with the flow rate of 0.18 mL min^{-1}. The solid residue was analyzed by FT-IR spectrophotometer, Spectrum One, Perkin Elmer, USA. The values of chemical oxygen demand (COD) in the samples were determined by Hach-Lange COD analyzing set, DR 2800 spectrophotometer and DRB 200 reactor, USA. Concentration of sulfate ions was determined by turbidimetric method [17] based on precipitation of sulfate ions in acid medium with barium chloride, forming barium sulfate crystals of uniform size. Light absorbance of the $BaSO_4$ suspension was measured by Hach 2100P Turbidimeter (USA).

2.5. Box–Behnken design and desirability function

Among RSM techniques, Box–Behnken design (BBD) is commonly chosen for the purpose of response optimization [19,20]. This is a three-level spherical design with excellent predictability particularly in cases when prediction of response at the extreme level is not the goal of the model.

Box–Behnken design with three numeric factors, varied over three levels (Table 2) was used to determine the operating conditions for maximizing the organic pollutant degradation, i.e., mineralization extent (final TOC content). Since one additional categorical factor, at two levels (Table 2), was involved, design was duplicated for each combination of the categorical factor levels, resulting in total of 34 experiments that were conducted under the conditions defined in Table 3, in random manner. A reduced cubic model was evaluated for the transformed response function, Eqs. (6) and (7):

$$\begin{aligned} Y' = {} & b_0 + b_1X_1 + b_2X_2 + b_3X_3 + \beta_1X_4 + b_{11}{X_1}^2 + b_{22}{X_2}^2 + b_{33}{X_3}^2 \\ & + b_{12}X_1X_2 + b_{13}X_1X_3 + \beta_{11}X_1X_4 + b_{23}X_2X_3 + \beta_{21}X_2X_4 \\ & + \beta_{31}X_3X_4 + \beta_{111}{X_1}^2X_4 + \beta_{122}X_1{X_2}^2 + \beta_{221}{X_2}^2X_4 \\ & + \beta_{331}{X_3}^2X_4 \end{aligned} \quad (6)$$

$$Y' = \ln\left[\frac{Y - \text{lower bound}}{\text{upper bound} - Y}\right] \quad (7)$$

where X_1, X_2, X_3, X_4 represent the factors in the model, b_n is the coefficient associated with each nth factor, and β_{ij} represents coefficients for categorical factor or their interactions with numerical factors. Combination of factors (such as X_1X_2) represents interactions between the individual factors in that term. Y and Y' represent the observed (final TOC content) and transformed response. Upper and lower bounds, 1939.2 and 4.51, respectively, were obtained by extending the range of observed responses for 1 (Table 3), in order to avoid zero in the equation. Obtained model and experimental data were analyzed statistically using *Design-Expert 6.0.6*, a DoE software tool from Stat-Ease, Inc.

Furthermore, desirability function has been one of the most important optimization techniques since the early eighties. Main reasons for this popularity might be counted as the convenience of the implementation of the method and its availability in many experimental design software packages [21]. Desirability function approach makes use of an objective function, $D(X)$, called the desirability function and transforms an estimated response into a scale free value (d_i) called desirability. The desirable ranges are from zero to one (least to most desirable, respectively). The factor settings with maximum total desirability are considered to be the optimal parameter conditions. The simultaneous objective function is a geometric mean of all transformed responses, Eq. (8):

$$D = (d_1 \times d_2 \times \cdots \times d_n)^{1/n} = \left(\prod_{i=1}^{n} d_i\right)^{1/n} \quad (8)$$

where n is the number of responses in the measure. If any of the responses falls outside the desirability range, the overall function becomes zero. The numerical optimization finds a point that maximizes the desirability function. Adjusting the importance the characteristics of a goal may alter. For several responses, all goals get combined into one desirability function. For simultaneous optimization, each response must have a low and high value assigned to each goal. The "Goal" field for responses must be one of five choices: "none", "maximum", "minimum", "target", or "in range" [22]. Factors are also included in the optimization at their design range by default, or as a maximum, minimum of target goal. In case of single-response optimization, it is determined how input parameters affect the desirability of individual response, d [23].

In this particular case, the most desired response value, i.e., goal parameter, was minimum observed response, i.e., minimum of transformed response, with highest importance. Accordingly, the meaning of goal parameter set for the purpose and corresponding desirability are presented below:

goal parameter is minimum	
if response < low value	$\Rightarrow d = 1$
as responses varies from low to high	$\Rightarrow 1 \geq d \geq 0$
if response > high value	$\Rightarrow d = 0$

Discussion on criteria settings for factors will be elaborated in detail in Sections 3.2 and 3.3.

3. Results and discussion

3.1. Experimental design analysis and results

The statistical study of the process was performed using response surface methodology (RSM), particularly by Box–Behnken

Table 2
Actual factors and their levels.

Type of factor	Parameter name	Code	Levels		
			1	2	3
Numerical			−1	0	1
	Mass weight of HCOONa, %	X_1	0.10	0.80	1.50
	Concentration of Fe-ions, [$Fe^{2+/3+}$], mol L^{-1}	X_2	0.01	0.11	0.20
	Concentration of H_2O_2, [H_2O_2], mol L^{-1}	X_3	0.11	1.16	2.20
Categorical			0	1	
	Type of Fe-salt	X_4	$FeSO_4{\cdot}7H_2O$	$FeCl_3{\cdot}6H_2O$	

Table 3
Design matrix and response at different factor levels.

		Factors				Response	Transformed response
Std.	Run	X_1, w(HCOONa), %	X_2, [$Fe^{2+/3+}$], mol L^{-1}	X_3, [H_2O_2], mol L^{-1}	X_4, type of Fe-salt	Y, TOC_{120}, mg L^{-1}	Y', ln[$(Y-4.51)/(1939.2-Y)$]
3	1	0.10	0.20	1.16	$FeSO_4{\cdot}7H_2O$	31.76	−4.248
31	2	0.80	0.11	1.16	$FeCl_3{\cdot}6H_2O$	568.3	−0.889
19	3	1.50	0.01	1.16	$FeCl_3{\cdot}6H_2O$	1752.6	2.237
32	4	0.80	0.11	1.16	$FeCl_3{\cdot}6H_2O$	498.3	−1.071
16	5	0.80	0.11	1.16	$FeSO_4{\cdot}7H_2O$	6.508	−6.875
9	6	0.80	0.01	0.11	$FeSO_4{\cdot}7H_2O$	926.4	−0.094
27	7	0.80	0.20	0.11	$FeCl_3{\cdot}6H_2O$	1473.0	1.147
10	8	0.80	0.20	0.11	$FeSO_4{\cdot}7H_2O$	1103.0	1.314
13	9	0.80	0.11	1.16	$FeSO_4{\cdot}7H_2O$	7.51	−6.468
17	10	0.80	0.11	1.16	$FeSO_4{\cdot}7H_2O$	**5.51**[a]	−7.567
21	11	1.50	0.20	1.16	$FeCl_3{\cdot}6H_2O$	936.4	−0.073
7	12	0.10	0.11	2.20	$FeSO_4{\cdot}7H_2O$	9.33	0.002
20	13	0.10	0.20	1.16	$FeCl_3{\cdot}6H_2O$	72.22	−3.317
6	14	1.50	0.11	0.11	$FeSO_4{\cdot}7H_2O$	1904.4	4.000
34	15	0.80	0.11	1.16	$FeCl_3{\cdot}6H_2O$	771.6	−0.420
30	16	0.80	0.11	1.16	$FeCl_3{\cdot}6H_2O$	650.8	−0.690
29	17	0.80	0.20	2.20	$FeCl_3{\cdot}6H_2O$	19.464	−4.855
14	18	0.80	0.11	1.16	$FeSO_4{\cdot}7H_2O$	7.02	−6.646
11	19	0.80	0.01	2.20	$FeSO_4{\cdot}7H_2O$	632.4	−0.733
23	20	1.50	0.11	0.11	$FeCl_3{\cdot}6H_2O$	**1938.2**[a]	7.567
28	21	0.80	0.01	2.20	$FeCl_3{\cdot}6H_2O$	675.6	−0.633
12	22	0.80	0.20	2.20	$FeSO_4{\cdot}7H_2O$	12.518	−5.483
2	23	1.50	0.01	1.16	$FeSO_4{\cdot}7H_2O$	1713.4	2.024
1	24	0.10	0.01	1.16	$FeSO_4{\cdot}7H_2O$	25.98	−4.490
25	25	1.50	0.11	2.20	$FeCl_3{\cdot}6H_2O$	1762	2.294
22	26	0.10	0.11	0.11	$FeCl_3{\cdot}6H_2O$	42.69	−3.905
4	27	1.50	0.20	1.16	$FeSO_4{\cdot}7H_2O$	61.14	−3.501
24	28	0.10	0.11	2.20	$FeCl_3{\cdot}6H_2O$	104.76	−2.907
15	29	0.80	0.11	1.16	$FeSO_4{\cdot}7H_2O$	6.14	−7.078
18	30	0.10	0.01	1.16	$FeCl_3{\cdot}6H_2O$	9.747	−5.909
5	31	0.10	0.11	0.11	$FeSO_4{\cdot}7H_2O$	54.96	−3.620
26	32	0.80	0.01	0.11	$FeCl_3{\cdot}6H_2O$	1256.4	0.606
8	33	1.50	0.11	2.20	$FeSO_4{\cdot}7H_2O$	15.23	−5.190
33	34	0.80	0.11	1.16	$FeCl_3{\cdot}6H_2O$	505.0	−1.053

[a] *Note*: Bolded values present bounds of observed range, used for transformation.

design. Individual parameters and their interaction effects on TOC reduction were determined and statistical predictive model of process was developed. Multiple regression analysis of experimental data, performed using Design-Expert software, resulted with model equation describing dependency of response (Y') to selected terms, meaning four process parameters and some of their interactions. Transformed response fitted well in a proposed reduced cubic model, Eq. (6).

For current study response surface model were evaluated using ANOVA (Table 4). F-value of 44.87 and p-value less than 0.0001 imply that the model is significant. The examination of residuals was used to investigate the model adequacy. Fig. 1 presents a normal probability plot of residuals for transformed response, Y'. As it can be seen, there is no severe indication of non-normality and neither any evidence pointing to possible outliers. Normal plot presented at Fig. 1 is normally distributed and resemble a straight line. Also, residuals are structureless and contain no obvious patterns, so it can be concluded that the model is adequate. Furthermore, residuals vs. predicted plot is also normally distributed and the equality of variance does not seem to be violated, as presented in Fig. 2. Obtained R^2 value, 0.9795, is close to one suggesting the fit is good and a variation in the observed value can be explained by the chosen model. Result of analysis shown in Fig. 3 is in accordance with given R^2 values. Namely, predicted vs. actual plot that shows equality of experimental data (actual) with the one obtained by the model (predicted) for the same initial values follows the line $x = y$. In an ideal case when R^2 valued would be 1, all points on predicted vs. actual graph would lie on the line $x = y$ [24,25]. The results obtained within this study prove the model adequacy and it can be concluded that the given model describes the investigated system very well throughout the experimental range.

Significance of each term in predictive model, evaluated by p-value less than 0.1000 is also presented in Table 4. Since coefficients for multi-level categorical factor (X_4) or their interactions with numerical factors (e.g., X_1X_4), β_{ij}, are not as simple to interpret, and do not have a physical, but only a mathematical meaning [23], these coefficients and equation in coded terms could not be used for interpretation of the model, yet real impression about process performance could be achieved from graphical interpretation of the model in accordance with model equation given in actual terms for each level of categorical factor.

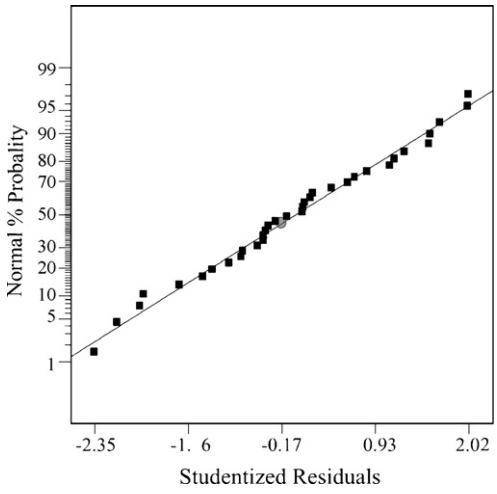

Fig. 1. Normal probability plot of residuals for transformed response.

Table 4
ANOVA results – model and coefficient validation: fit summary.

Source	Sum of squares	Degrees of freedom	*F*-Value	*p*-Value	R^2
Model	416.46	17	44.87	<0.0001	0.9795
X_1	78.73	1	144.22	<0.0001	
X_2	10.67	1	19.55	0.0004	
X_3	54.29	1	99.45	<0.0001	
X_4	93.09	1	170.53	<0.0001	
X_1^2	8.15	1	14.94	0.0014	
X_2^2	4.51	1	8.26	0.0110	
X_3^2	31.12	1	57.00	<0.0001	
X_1X_2	14.23	1	26.07	0.0001	
X_1X_3	21.42	1	39.23	<0.0001	
X_1X_4	9.58	1	17.55	0.0007	
X_2X_3	12.20	1	22.35	0.0002	
X_2X_4	2.46	1	4.50	0.0499	
X_3X_4	2.59	1	4.75	0.0446	
$X_1^2X_4$	3.10	1	5.68	0.0299	
$X_1X_2^2$	2.60	1	4.76	0.0445	
$X_2^2X_4$	35.40	1	64.84	<0.0001	
$X_3^2X_4$	4.28	1	7.84	0.0128	
Total	425.19	33	–	–	
Residual error lack-of-fit	2.71	8	1.53	0.1749	

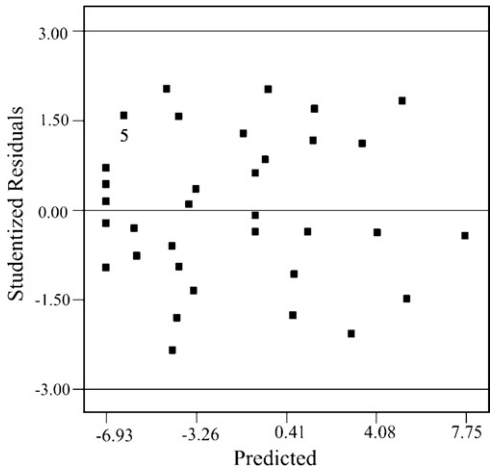

Fig. 2. Residuals vs. predicted plot for transformed response.

Therefore, predictive model given in actual terms regarding transformed response Y', i.e., $\ln[(TOC_{120} - 4.51)/(1939.2 - TOC_{120})]$, is stated bellow, Eq. (9). Since each combination of categorical levels has an equation that predicts the response, two equations are presented:

$$\ln\left[\frac{TOC_{120} - 4.51}{1939.2 - TOC_{120}}\right]_{Fe(II)\,sulfate} = -1.25 + 1.47 \times w(HCOONa) - 68.47 \times [Fe^{2+}] - 4.63 \times [H_2O_2] + 3.25 \times w(HCOONa)^2 + 410.29 \times [Fe^{2+}]^2 + 2.41 \times [H_2O_2]^2 + 6.73 \times w(HCOONa) \times [Fe^{2+}] - 2.23 \times w(HCOONa) \times [H_2O_2] - 12.44 \times [Fe^{2+}] \times [H_2O_2] - 127.53 \times w(HCOONa) \times [Fe^{2+}]^2 \quad (9a)$$

$$\ln\left[\frac{TOC_{120} - 4.51}{1939.2 - TOC_{120}}\right]_{Fe(III)\,chloride} = -7.01 + 7.64 \times w(HCOONa) + 35.20 \times [Fe^{3+}] - 0.84 \times [H_2O_2] + 0.77 \times w(HCOONa)^2 - 44.06 \times [Fe^{3+}]^2 + 1.11 \times [H_2O_2]^2 + 6.73 \times w(HCOONa) \times [Fe^{3+}] - 2.23 \times w(HCOONa) \times [H_2O_2] - 12.44 \times [Fe^{3+}] \times [H_2O_2] - 127.53 \times w(HCOONa) \times [Fe^{3+}]^2 \quad (9b)$$

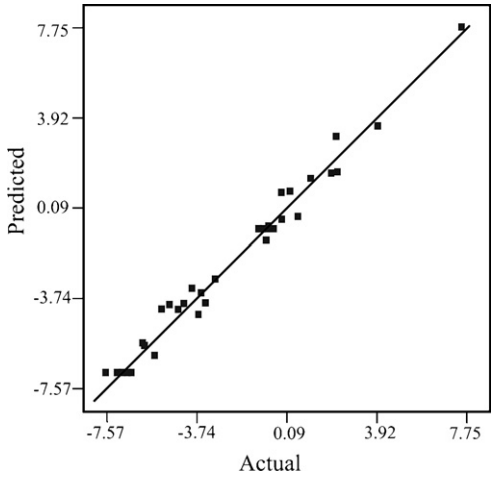

Fig. 3. Predicted vs. actual plot for transformed response.

Graphical interpretation of the model is shown on Fig. 4a–c, taking into consideration responses for each type of oxidant used and average responses.

3.2. Overview of applied process

It can be seen (Table 3; Fig. 4) that the highest mineralization extents were achieved when Fe^{2+} (Fe(II) sulfate salt) is used as a catalyst. Performance of classic Fenton process is very good even in case of the highest organic load, as in case of SIM3, where the initial TOC content is 5500 mg L^{-1}. Desirable mineralization extent could be maintained within the following conditions: rather low initial concentration of ferrous ions and catalyst/oxidant ratios (Fe/H_2O_2) from 1:10 to 1:55. As mentioned in Section 1, Fenton's oxidation is the most effective at pH values near 3. Since consistent generation of ferric hydroxo complexes is observed between pH 3 and 7, the initial pH was adjusted at 3.5 as a compromise solution regarding

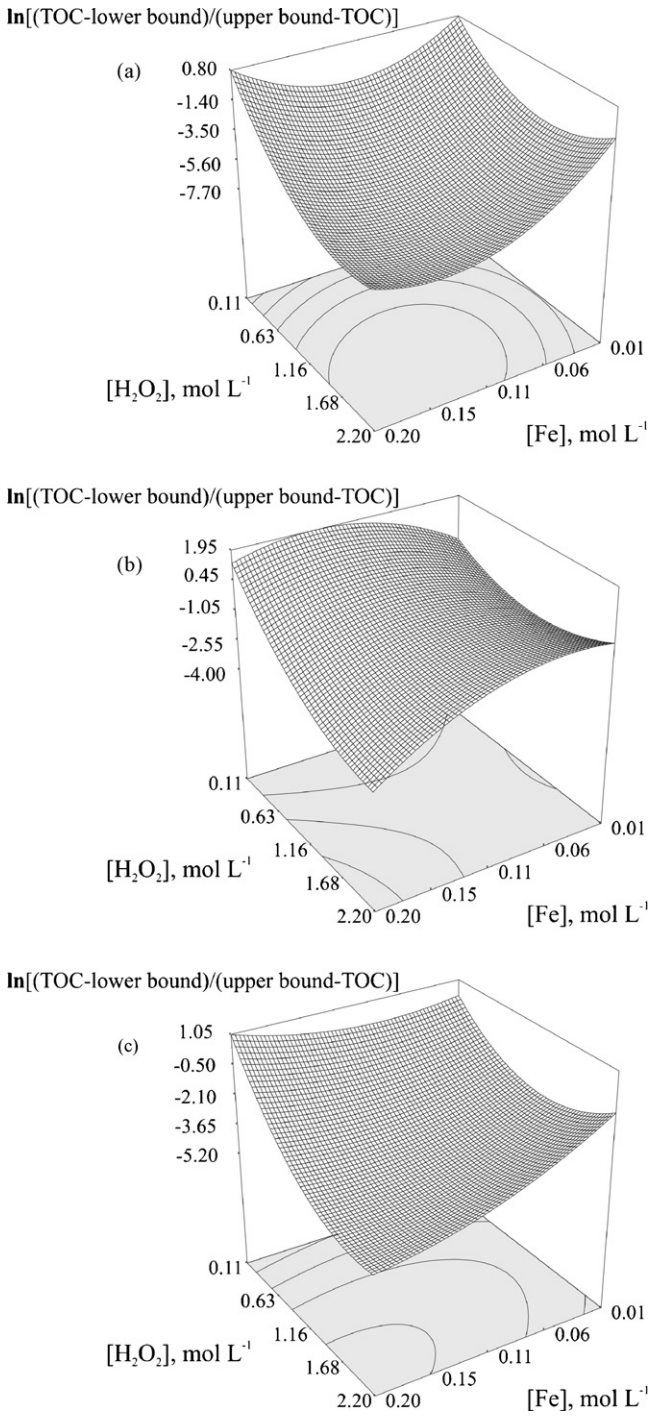

Fig. 4. (a–c) Graphical interpretation of the model that describes dependency of mineralization extent in terms of transformed response to process parameters and their interactions.

high oxidation extent and formation of small flocs leading towards sludge production.

Furthermore, the formation and consecutive presence of the carboxyl radical, $CO_2^{\bullet-}$, Eqs. (4) and (5a) is also important due to the impact on mineralization in great extent. It can be concluded that the cleavage of formate towards CO_2 is self-catalyzed process. Production of oxalic acid, Eq. (5b), was also observed and its final concentration in the system was determined (Table 5).

Although Fenton process appeared to be an effective technology for the treatment of wastewater, the resulted sludge usually contains heavy metals and different inorganic anions initially present

Table 5
Characteristics of system treated by optimized process, Fe^{2+}/H_2O_2: $[Fe^{2+}] = 0.05\ mol\ L^{-1}$, $[H_2O_2] = 1.00\ mol\ L^{-1}$, pH 3.5, time of reaction 120 min.

	Initial	Final
Supernatant		
TOC, mg L^{-1}	2,930	18.22[b]
IC, mg L^{-1}	11,850	65.18
COD, mg L^{-1}	3,966	1000
w(HCOOH), %	0.8	0.003
$w(H_2C_2O_4)$, %	–	0.004
$[H_2O_2]$, mol L^{-1}	1.0	0.03
$[Fe^{2+}]$, mol L^{-1}	0.05	0.001
$[Fe^{3+}]$, mol L^{-1}	0	0.008
$\gamma(SO_4^{2-})$, g L^{-1}	77	13
κ, mS cm^{-1}	103	86
pH	3.5	1.9
Solid residue		
m_F, g/100 mL	–	0.7

[b] *Note*: Developed BBD model predicted a value of 17.33 mg L^{-1}.

on the liquid phase [26]. In case of studied simulated systems, residue could contain sodium salts, due to high content of sodium ions and different anions in the system: iron, sulfate ions and different Fe-chelating compounds, e.g., Fe-oxalate, since oxalate were produced by the recombination of $CO_2^{\bullet-}$ radicals.

FT-IR spectroscopy has been used to gain the superficial understanding of the residue characteristics [27–30]. As shown in Fig. 5, peaks between 3600 and 2900 cm^{-1} are characteristic of the stretching bonds of O—H, which can be found in some possible compounds: formic acid, HCOOH, since it could be easily formed from formate ions in highly acidic conditions and ferric hydroxo complexes, $[Fe(OH)_n(H_2O)_y]^{3-n}$. These complexes would also behave as a coagulant in aqueous phase, thus increasing the sludge production. The peak observed at 2100 cm^{-1} indicates the O—H overtone. Peaks appeared at ≈1650 cm^{-1} are assigned to the C=O bonds, once again found in oxalate and formate. Wide band from 1200 to 950 cm^{-1} responds to stretching frequencies of S—O and C—O bonds. These bonds could be found in different Fe-chelating sulfato complexes, $[Fe(L)SO_4]^{n-}$, where ligand, L, could be oxalate, water or carbonate ion, respectively [29]. Somewhat distinct peak at ~700 cm^{-1} depicted O—C=O in-plane deformation (rocking vibration) inside formate, while peaks found between 700 and 600 cm^{-1} respond to O—C=O bending vibration [28]. Other possible compound formed during the process is Fe-bis(oxalato) complex, $[Fe(C_2O_4)_2]^{2-}$, with following assignments in IR spectra: C=O stretching at ~1650 cm^{-1}, C—C and C—O stretching at ~1300 cm^{-1} ranging to 900 cm^{-1}, O—C=O bending and rocking vibrations at ~700 cm^{-1} and finally, Fe—O stretching at 500–450 cm^{-1} [28,30]. The presence of inorganic compounds in

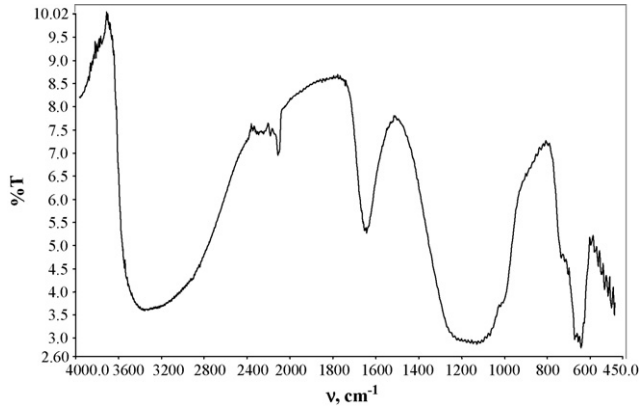

Fig. 5. FT-IR spectra of Fenton's solid residue.

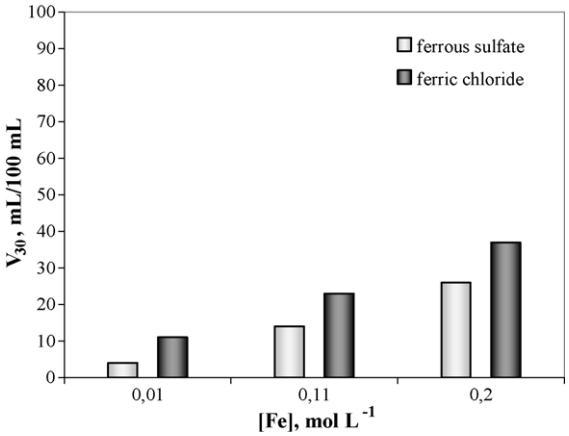

Fig. 6. Average production of residual sludge depending on the initial concentration, [$Fe^{2+/3+}$], and type of iron salt.

residue could also be approved by FT-IR. Namely, sodium sulfate and sodium carbonate manifest with bands at ~600 cm^{-1}.

Furthermore, required separation, treatment and disposal of residue, increase the overall cost. On the other hand, process optimization could contribute in lowering down the sludge production. As it can be seen from Fig. 6, application of ferrous sulfate resulted in less residue compared with the experiments where ferric chloride was used. Also, finding and a certain point in design space that results with reasonable efficiency in terms of mineralization at lower concentration of iron, [Fe^{2+}], presents a specific goal.

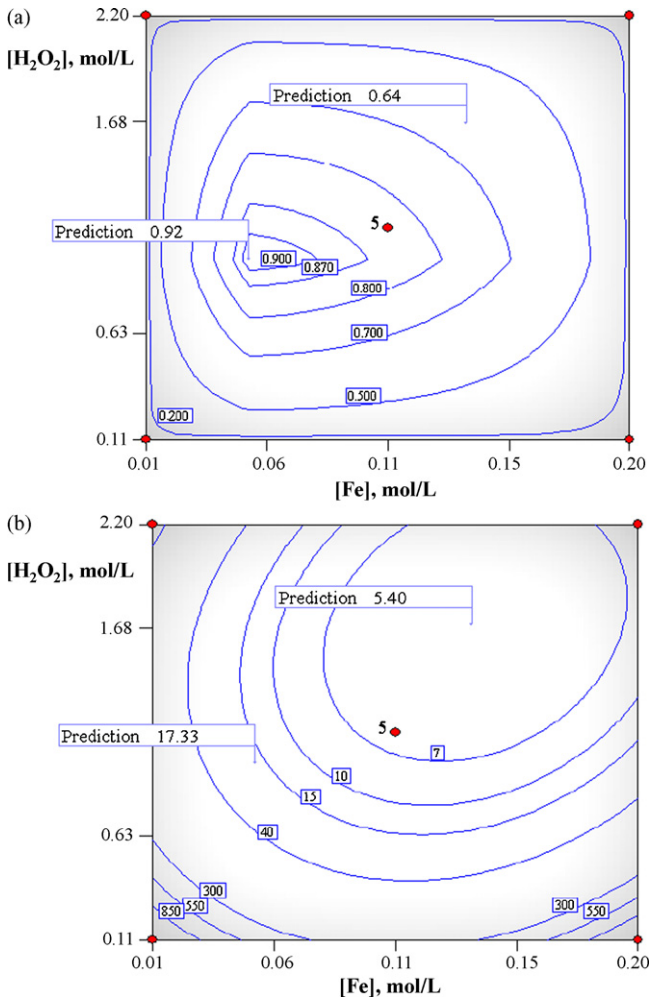

Fig. 7. Result of numerical optimization – contour plots for result of (a) desirability function and (b) predicted response, *Y*, final TOC content.

3.3. Single-response optimization using desirability function

Single-response optimization caters to optimization of single response, i.e., TOC content in system SIM2, and determines how input parameters affect the desirability of individual response. System SIM2 was chosen for further optimization since the organic loads (TOC) in this type of real wastewaters usually vary around 3000 mg L^{-1}. Contour plot for desirability was first drawn keeping input parameters in range and response (TOC content) at minimum. Furthermore, an optimal design point was achieved by adjusting the settings for input parameters while TOC content was kept at minimum. Desired settings for input parameters, i.e., criteria were as follows: [Fe^{2+}] as target of 0.5 mol L^{-1} – in order to avoid high production of sludge: [H_2O_2] as target of 1.0 mol L^{-1} to maintain compromising catalyst/oxidant ration of 1:20. As it can be seen from Fig. 7a and b, an optimal design point resulted with desirability of 0.92 according to set criteria. In this particular point in design space, predicted response was 17.33 mg L^{-1}, not far from predicted minimum (5.41 mg L^{-1}), considering the TOC initial value (Table 1.).

Additional experiment with optimized conditions was performed. Initial and final characteristics of the studied system were shown in Table 5. Observed TOC value, 18.22 mg L^{-1} confirmed what it was predicted. Also, process resulted in a minor amount of solid residue, 0.7 g/100 mL. Furthermore, decrease in concentration of Fe and sulfate ions correspond with formation of sludge containing different complexes (Section 3.2).

4. Conclusion

Pre-treatment of simulated industrial wastewaters (SIM1, SIM2 and SIM3) containing organic and inorganic compounds (1,2-dichloroethane, sodium formate, sodium hydrogen carbonate, sodium carbonate and sodium chloride) by oxidative degradation using homogeneous Fenton type processes (Fe^{2+}/H_2O_2 and Fe^{3+}/H_2O_2) has been evaluated. RSM Box–Behnken design was applied. Four factors have been examined, including initial content of sodium formate (X_1), initial Fe^{2+}/Fe^{3+} concentration (X_2), initial hydrogen peroxide concentration (X_3), and finally, categorical factor (X_4), type of used iron salt, ferrous sulfate and ferric chloride.

Using statistical analysis of the applied processes, where up to 94% of initial TOC was removed after 120 min, the following were noticed: (i) among applied salts, ferrous sulfate was found to be most appropriate; and (ii) the optimal reagent doses for reducing the pollutant content, in terms of TOC removal and sludge production were assessed for applied process using desirability function approach. From the results obtained in this study, it can be concluded that the given predictive model described the studied systems very well and satisfactory throughout the investigated range, evaluated by the analysis of variance analysis, ANOVA. Implementation of predictive model equations in numerical optimization resulted in successful determination of design space.

The presented approach showed that classic Fenton process has a certain potential for its industrial application as a pre-treatment phase of wastewater treatment.

Acknowledgments

This work was financially supported by The National Foundation for Science, Higher Education and Technological Development of the Republic of Croatia, in the frame of the Project #04/14, *Wastewater Treatment in DINA-Petrokemija Omišalj as a Contribution*

to Ecosystem Preservation. We are especially grateful for successful cooperation with MSc Jarolim Meixner, Department of Environmental Protection, DINA-Petrokemija Inc., Omišalj, Croatia.

References

[1] R.L. Droste, Theory and Practice of Water and Wastewater Treatment, John Wiley & Sons, Environmental Engineering and Science, New York, 1997.
[2] J.H. Ramirez, C.A. Costa, L.M. Madeira, Experimental design to optimize the degradation of the synthetic dye Orange II using Fenton's reagent, Catal. Today 107–108 (2005) 68–76.
[3] H.Y. Shu, M.C. Chang, H.J. Fan, Decolorization of azo dye acid black 1 by the UV/H_2O_2 process and optimization of operating parameters, J. Hazard. Mater. 113 (2004) 201–208.
[4] J. Levec, Wet oxidation processes for treating industrial wastewaters, Chem. Biochem. Eng. Q. 11 (1997) 47–58.
[5] M. Muruganandham, M. Swaminathan, Decolourisation of reactive Orange 4 by Fenton and photo-Fenton oxidation technology, Dyes Pigments 63 (2004) 315–321.
[6] D.R. de Souza, E.T. Fleury Mendonça Duarte, G. de Souza Girardi, V. Velani, A.E. da Hora Machado, C. Sattler, L. de Oliveira, J.A. de Miranda, Study of kinetic parameters related to the degradation of an industrial effluent using Fenton-like reactions, J. Photochem. Photobiol. A 179 (2006) 269–275.
[7] A. Lopez, M. Pagano, A. Volpe, A.C. Di Pinto, Fenton's pre-treatment of mature landfill leachate, Chemosphere 54 (2004) 1005–1010.
[8] J.M. Chacón, M.T. Leal, M. Sánchez, E.R. Bandala, Solar photocatalytic degradation of azo-dyes by photo-Fenton process, Dyes Pigments 69 (2006) 144–150.
[9] R.S. Gupta, Environmental Engineering and Science, An Introduction, Government Institutes, Rockville, 1997.
[10] E. Neyens, J. Baeyens, A review of classic Fenton's peroxidation as an advanced oxidation technique, J. Hazard. Mater. 98 (2003) 33–50.
[11] P. Wardman, Reduction potentials of one-electron couples involving free radicals in aqueous solution, J. Phys. Chem. Ref. Data 18 (1989) 1637–1755.
[12] P. Neta, M. Simic, E. Hayon, Pulse radiolysis of aliphatic acids in aqueous solutions I. Simple monocarboxylic acids, J. Phys. Chem. 73 (1969) 4207–4213.
[13] G.V. Buxton, R.M. Sellers, Acid dissociation-constant of carboxyl radical-pulse-radiolysis studies of aqueous-solutions of formic-acid and sodium formate, J. Chem. Soc. Faraday Trans. 1 (69) (1973) 555–559.
[14] M. Lin, Y. Katsumura, Y. Muroya, H. He, T. Miyazaki, D. Hiroishi, Pulse radiolysis of sodium formate aqueous solution up to 400 °C: absorption spectra, kinetics and yield of carboxyl radical $CO_2^{\bullet -}$, Radiat. Phys. Chem. 77 (2008) 1208–1212.
[15] P.K. Malik, S.K. Saha, Oxidation of direct dyes with hydrogen peroxide using ferrous ion as catalyst, Sep. Purif. Technol. 31 (2003) 241–250.
[16] S. Meric, D. Kaptan, T. Olmez, Color and COD removal from wastewater containing Reactive Black 5 using Fenton's oxidation process, Chemosphere 54 (2004) 435–441.
[17] APHA, Standard Methods for the Examination of Water and Wastewater Treatment, 20th ed., American Public Health Association, Washington, DC, USA, 1998.
[18] R.F.P. Nogueira, M.C. Oliveira, W.C. Paterlini, Simple and fast spectrophotometric determination of H_2O_2 in photo-Fenton reactions using metavanadate, Talanta 66 (2005) 86–91.
[19] S. Ray, RSM: a statistical tool for process optimization, Ind. Tex. J. 117 (2006) 24–30.
[20] S. Bae, M. Shoda, Statistical optimization of culture conditions for bacterial cellulose production using Box–Behnken design, Biotechnol. Bioeng. 90 (2005) 20–28.
[21] C.S. Aksezer, On the sensitivity of desirability functions for multiresponse optimization, J. Ind. Manage. Optim. 4 (2008) 685–696.
[22] A. Aggarwal, H. Singh, P. Kumar, M. Singh, Optimization of multiple quality characteristics for CNC turning under cryogenic cutting environment using desirability function, J. Mater. Process. Technol. 205 (2008) 42–50.
[23] R.H. Myers, D.C. Montgomery, Response Surface Methodology. Process and Products Optimization Using Designed Experiments, John Wiley & Sons Inc., New York, 2002.
[24] R. Molina, F. Martínez, J.A. Melero, D.H. Bremner, A.G. Chakinala, Mineralization of phenol by a heterogeneous ultrasound/Fe-SBA-15/H_2O_2 process: multivariate study by factorial design of experiments, Appl. Catal. B: Environ. 66 (2006) 198–207.
[25] I. Grčić, M. Mužic, D. Vujević, N. Koprivanac, Evaluation of atrazine in UV/FeZSM-5/H_2O_2 system using factorial experimental design, Chem. Eng. J. 150 (2009) 476–484.
[26] C.T. Benatti, A.C.S. da Costa, C.R. Granhen Tavares, Characterization of solids originating from the Fenton's process, J. Hazard. Mater. 163 (2009) 1246–1253.
[27] T.J. Smith, J.E. Kennedy, C.L. Higginbotham, The rheological and thermal characteristics of freeze-thawed hydrogels containing hydrogen peroxide for potential wound healing applications, J. Mech. Behav. Biomed. Mater. 2 (2009) 264–271.
[28] E. Pretsch, J. Seibl, W. Simon, T. Clerc, Tabellen zur Strukturaufklaerung Organisher Verbindungen mit Spektroskopischen Methoden, Springer Verlag, Berlin, 1981.
[29] K. Nakamoto, P.J. McCarthy, Spectroscopy and Structure of Metal Chelate Compounds, John Wiley & Sons, New York, 1968.
[30] Freeman F. Bentley, Lee D. Smithson, Adele L. Rozek, Infrared Spectra and Characteristic Frequencies, ~700–300 cm^{-1}, A Collection of Spectra, Interpretation, and Bibliography, John Wiley & Sons, Inc., USA, 1968.